Original Article

Normal Skeletal Standardized Uptake Values Obtained from Quantitative Single-Photon Emission Computed Tomography/Computed Tomography: Time-Dependent Study on Breast Cancer Patients

Amit Nautiyal[1,2], Ashish Kumar Jha[1,2], Sneha Mithun[1,2], Viraj Sawant[1,2], Raveena Jadhav[1,2], Kranti Khairnar[1,2], Venkatesh Rangarajan[1,2]

[1]Department of Nuclear Medicine and Molecular Imaging, Tata Memorial Centre, [2]Homi Bhabha National Institute, Mumbai, Maharashtra, India

Abstract

Aim: To estimate the standard uptake values (SUVs) of Tc-99m methylene-diphosphonate (Tc-99m MDP) from normal skeletal sites in breast cancer patients using quantitative single-photon emission computed tomography (SPECT). **Materials and Methods:** A total of 60 breast cancer patients who underwent Tc-99m MDP SPECT/CT study at different postinjection acquisition times were included in this study. Based on postinjection acquisition time, patients were divided into four study groups (n_15 each), i.e. Ist (2 h), IInd (3 h), IIIrd (4 h), and IVth (5 h). Image quantification (SUVmax and SUVmean) was performed using Q.Metrix software. Delineation of volume of interest was shaped around different bones of the skeletal system. **Results:** The highest normal SUVmax and SUVmean values were observed in lumber and thoracic vertebra (8.89 ± 2.26 and 2.89 ± 0.58) for Group I and in pelvis and thoracic (9.6 ± 1.32 and 3.04 ± 0.64), (10.93 ± 3.91 and 3.65 ± 0.97), (11.33 ± 2.67 and 3.65 ± 0.22) for Group II, III and IV, respectively. Lowest normal SUVmax and SUVmean values were observed in humerus and ribs (3.22 ± 0.67 and 0.97 ± 0.18), (5.16 ± 1.82 and 1.18 ± 0.16) for Group I, IV, and in humerus (3.17 ± 0.58 and 0.85 ± 0.26), (3.98 ± 1.12 and 1.04 ± 0.28) for Group II and III, respectively. Significant difference ($P < 0.05$) noted in SUVmax for sternum, cervical, humerus, ribs, and pelvis with respect to time. However, significant difference ($P < 0.05$) noted in SUVmean for all skeletal sites with respect to time. **Conclusions:** Our study shows variability in normal SUV values for different skeletal sites in breast cancer patients. Vertebral bodies and pelvis contribute highest SUV values. Time dependency of SUVs emphasizes the usefulness of routinely acquired images at the same time after Tc-99m MDP injection, especially in follow-up studies.

Keywords: *Bone uptake, breast cancer, quantitative single-photon emission computed tomography/computed tomography, standard uptake values single-photon emission computed tomography, Tc-99m methylene-diphosphonate*

Introduction

Over the last many years, Tc-99m methylene diphosphonate (Tc-99m MDP) has been widely used as a bone scintigraphy agent in the diagnosis of many pathological conditions such as metastatic bone disease, stress fractures, degenerative changes, or other similar conditions.[1-3] It is known that skeletal metastases often happen with breast cancer.[4,5] Tc-99m MDP rapidly enters into extracellular fluid after intravenous injection and is immediately taken up by the bone, where it binds with the hydroxyapatite mineral component of the osseous matrix by the process of chemisorption.[5] Gamma camera is a widely used instrument in nuclear medicine which uses two-dimensional planar imaging for qualitative analysis of the uptake of tracer in bone tissue. However, due to the lack of depth information in planar whole-body scans, it is a difficult task to estimate the absolute value of tracer uptake from bone tissues. Later single-photon emission computed tomography (SPECT) was used in quantitative analysis of tracer uptake in bone tissue, where images were obtained from a fixed range of body and have been interpreted using the relative intensity of tracer uptake instead of quantitative analysis of tracer concentration.[6] This problem was overcome by the technical development and wide acceptance of integrated Single SPECT/computed tomography (SPECT/CT) system made it clinically useful for the quantification.[3,7-12]

How to cite this article: Nautiyal A, Jha AK, Mithun S, Sawant V, Jadhav R, Khairnar K, *et al.* Normal skeletal standardized uptake values obtained from quantitative single-photon emission computed tomography/computed tomography: Time-dependent study on breast cancer patients. Indian J Nucl Med 2021;36:398-411.

Address for correspondence:
Dr. Venkatesh Rangarajan, Department of Nuclear Medicine and Molecular Imaging, Tata Memorial Hospital, Tata Memorial Centre, Dr. Ernest Borges Road, Parel, Mumbai - 400 012, Maharashtra, India.
E-mail: drvrangarajan@gmail.com

Received: 08-04-2021
Revised: 14-08-2021
Accepted: 31-08-2021
Published: 15-12-2021

Access this article online

Website: www.ijnm.in

DOI: 10.4103/ijnm.ijnm_47_21

Quick Response Code:

Quantitative SPECT allows the estimation of standardized uptake values (SUVs), which can be used for the staging of disease and follow-up assessment.[13] SUV is a semi-quantitative parameter, frequently used for the quantification of uptake of tracer.[13,14] It is defined as the ratio of activity per unit volume of interest (VOI) to the activity per unit whole body volume.[5,11] The SUV can be measured as patient's body weight (SUVbw), lean body mass (SUVlbm), or body surface area (SUVbsa).[8,14] Concerning SUV measurement, however, SPECT/CT has not been exploited as much as positron emission tomography/CT (PET/CT). In PET/CT, SUV is widely been used for quantification purposes.[15-19] The overall effective dose received by the patient from standard ^{18}F NaF PET/CT scans is higher as compared to Tc-99m MDP bone scan.[20] Besides, the easy availability and cost-effectiveness of Tc-99m MDP make it ideal for clinical use as compared to F-18 NaF.[21]

Although to establish and use quantitative SPECT as a biomarker to differentiate benign from malignant bone disease, it is important to determine the normal SUV values for each one of the skeletal systems. In PET/CT, normal SUV values for different skeletal sites are already established.[22,23] However, due to the lack of popularity and standardization of SPECT/CT system, very few studies were performed to quantify and establish the normal SUV values for different skeletal sites in breast cancer patients.[9,24] The impact of postinjection acquisition time on SUV has already been studied in PET/CT.[25-27] However, there is no study has been reported the possible impact of imaging time on SUV values obtained using quantitative SPECT/CT with Tc-99m MDP.

The primary aim of our study was to estimate the SUV value from normal bones or skeletal sites in breast cancer patients using Tc-99m MDP-SPECT/CT bone scans. Moreover, postinjection acquisition time-dependent changes in SUV values were also studied. Furthermore, the correlation between SUVs and patient parameters such as age, body mass index (BMI), administered activity, and alkaline phosphatase (ALP) was also evaluated.

Materials and Methods

Patients

This retrospective study was performed on patients who underwent for Tc-99m MDP SPECT/CT bone scan at our center between Jun 2019 and March 2020. A total of 60 female patients (mean age, 46.93 ± 10.92 years; age range, 28–81 years) were enrolled for the study. Patients' data were retrieved from the hospital picture archiving and communication system. All these patients were positively diagnosed with breast cancer by breast biopsy. The clinical indication of referred patients for the bone scan was either initial staging or routine follow-up with breast cancer. The injected activity of Tc-99m MDP ranged from 900.21 MBq (24.33 mCi) to 948.21 MBq (25.62 mCi) (mean, 922.27 ± 10.98 MBq). Patients were divided into four groups (n_15 each) based on postinjection acquisition time, i.e. Ist (2 h), IInd (3 h), IIIrd (4 h), and IVth (5 h). Detailed patient characteristics of each group are mentioned in Table 1.

All patients were selected based on the following inclusion criteria: (1) a SPECT/CT procedure from head to lower thigh was conducted at above-mentioned time points after intravenous Tc-99m MDP administration (2) normal ALP and creatinine level (3) did not receive chemotherapy, radiotherapy, and radioimmunotherapy recently (4) absence of skeletal metastasis or any kind of degenerative changes on skeletal sites.

Quantitative single-photon emission computed tomography/computed tomography

The study was performed using a SPECT/CT system (Discovery NM/CT 670 Pro; GE Healthcare, Israel) equipped with a low-energy high-resolution collimator at four different acquisition time points postintravenous injection of Tc-99m MDP. All patients were well prepared as per the international guidelines before SPECT/CT procedure.[28] Acquisition and reconstruction parameters were the same for all imaging groups. Detailed technical parameters of examination are mentioned in Table 2. In addition, all data were corrected with scatter correction based on scatter window subtraction, depth-dependent resolution recovery, and attenuation correction using an attenuation map derived from the CT scan. These all corrections were performed in the vendor-supplied software (Volumetrix MI, GE Healthcare). Moreover, a post-OSEM reconstruction butterworth filter (critical frequency of 0.48 and power of 10) was also applied.

Sensitivity measurement

To convert measured counts of a region of interest into activity, the sensitivity of SPECT/CT gamma camera was evaluated. Sensitivity was measured as recommended by a vendor using

Table 1: Patient characteristics

Parameter	SPECT/CT imaging groups			
	I (2 h)	II (3 h)	III (4 h)	IV (5 h)
Patients (*n*)	15	15	15	15
Age (years)	46.66±10.04 (33-68)	45.4±6.68 (36-56)	44.06±9.56 (28-64)	51.6±15.19 (26-81)
BMI	22.38±2.94	21.92±2.97	21.54±2.91	22.63±2.67
ALP (IU/L)	77.6±16.11	78.26±9.42	75.26±13.81	80.26±16.75
Creatinine (mg/dL)	0.69±0.14	0.65±0.11	0.66±0.11	0.67±0.10

Results displayed as mean±SD (range). BMI: Body mass index, ALP: Alkaline phosphatase, SD: Standard deviation, SPECT/CT: Single-photon emission computed tomography/computed tomography

a Petri dish which was filled with a solution of 80 MBq (2.16 mCi) Tc-99m pertechnetate and saline. This petri dish is positioned on the foam holder and placed over the center of first detector. At the same distance of dish, the second detector was also placed as the first detector. The acquisition was performed with a 140% ± 10% energy window and matrix size of 256 × 256 and stopped when 4 million counts were acquired on both detectors. Thereafter, camera sensitivity was estimated by the vendor specified formula.[29]

Table 2: Technical parameters of single-photon emission computed tomography/computed tomography examination

Collimator	LEHR
SPECT	
Energy window	140±10%
Scatter window	120±10%
Bed positions	3
Acquisition mode	Step and shoot
Matrix size	128×128
Number of projections	60
Time per view (s)	10
Angular increment (degree)	6
Reconstruction (iterations and subsets)	OSEM (2 and 10)
CT	
kVp	120
mAs	70
Slice thickness (mm)	5
Tube rotation time (s)	0.5
Matrix size	512×512
Reconstruction	ASiR

SPECT: Single photon emission computed tomography, LEHR: Low energy high resolution, OSEM: Ordered subset expectation maximization, ASiR: Adaptive statistical iterative reconstruction, CT: Computed tomography

$$Sensitivity = \frac{N}{T} \Big/ \frac{A}{D}$$

Where N = total number counts in the image, D = decay correction factor between dose measurement time and acquisition time, T = acquisition time, and A = administered activity. The resulting system sensitivity was 160 counts per min per microcurie.

Image quantification

Image quantification was performed using Q.Metrix software (supplied by GE Healthcare), which converted activity concentration values into SUV. After processing, data were loaded into the software. Information regarding acquisition parameters, camera sensitivity, patient information, administered activity, and scan time was entered into Q.Metrix software [Figure 1]. SUVs were measured in the unit of body weight (BW) g/ml. These measured SUV values of Tc-99m MDP were demonstrated as SUV maximum (SUVmax) and SUV mean (SUVmean). The SUVmax was defined as the pixel value with the highest activity concentration within a VOI, whereas SUVmean was the mean pixel value of activity concentration within the VOI sampled:

$$SUV_{max} = \frac{\text{Maximum Activity/Voxel\_vol}}{\text{Decay corrected administered activity/BW}}$$

$$SUV_{mean} = \frac{\text{Total Activity/Vol\_vol}}{\text{Decay corrected administered activity/BW}}$$

A manual delineation technique opted for SUV measurement. Delineation of VOI was made around visually normal skeletal sites of SPECT/CT images: Skull, scapula, sternum, ribs, cervical spine, thoracic spine,

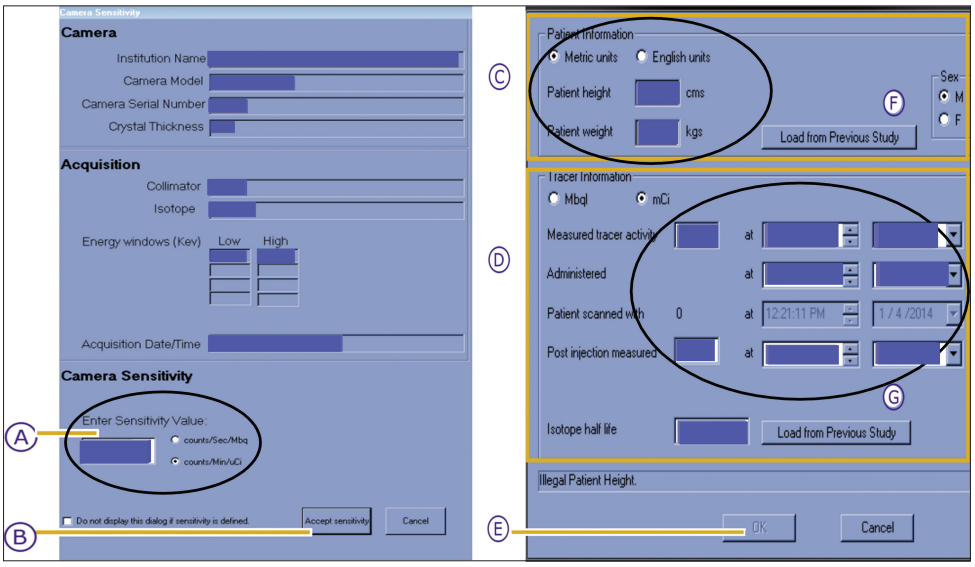

Figure 1: Q.Metrix processing; enter camera sensitivity (a), accept sensitivity (b), enter patient information (c), enter tracer information (d), accept all (e), load patient information from previous study (f) and load tracer information from previous study (g)

lumbar spine, pelvis, humerus, and femur. The size of VOI was carefully monitored in all image sections (axial, sagittal, and coronal) of the bone [Figure 2].

Statistical analysis

All statistical analyses were performed using Origin Pro 2019 (OriginLab Corp., Northampton, MA, USA). All patient parameters and SUV data were presented as the mean ± standard deviation. The coefficient of variation (COV) was used to measure the degrees of dispersion of the SUVmean and SUVmax for above-mentioned skeletal sites. The relationship of SUVmax and SUVmean with the patient's age, BMI, administered activity, and ALP was evaluated using the Pearson correlation coefficient. Demographic and injection parameters of all groups were compared using Kruskal–Wallis ANOVA test. For each skeletal site, the differences in SUVs between the imaging groups were also compared using Kruskal–Wallis ANOVA test, whereas $P < 0.05$ was considered statistically significant. Box and whisker plot was used to display the spread and distribution of SUVs for different imaging groups. The top and bottom of the boxes represented the first and third quartile, whereas the end of whiskers represented minimum and maximum values of data. The median value was indicated by a line in the box, whereas the mean value was indicated by a rectangular marker inside the box.

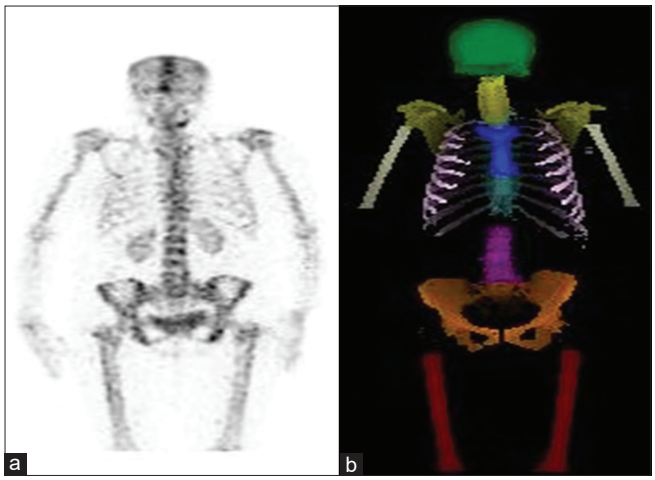

Figure 2: (a) Tc-99m methylene-diphosphonate single-photon emission computed tomography/computed tomography maximum intensity projection image and (b) 3D volume segmentation for different bone parts

Results

A total of 60 patients having a history of breast cancer were divided into four groups, i.e. Ist (2 h), IInd (3 h), IIIrd (4 h), and IVth (5 h) based on postinjection acquisition time (for each group; n = 15). The characteristics of patients in each group are listed in Table 1. However, no significant difference in patients age, BMI, ALP, creatinine, and administered activity between all four groups was noted (P = 0.46, 0.89, 0.84, 0.82, and 0.99, respectively). Comparisons of different demographic and clinical parameters of all groups are mentioned in Table 3. The box and whisker plots of parameters between all four groups are shown in Figure 3.

We have observed different normal SUVmax and SUVmean values for various skeletal sites [Figures 4 and 5]. Overall, study results show that thoracic, lumbar, and pelvis exhibit the highest SUVmax and SUVmean values as compared to rest skeletal sites. However, the lowest SUVmax and SUVmean values among all skeletal sites were observed in humerus and ribs, respectively. The highest values of the SUVmax and SUVmean among all of the skeletal sites were observed in lumber and thoracic vertebra (8.89 ± 2.26 and 2.89 ± 0.58) for Group I and in the pelvis and thoracic (9.6 ± 1.32 and 3.04 ± 0.64), (10.93 ± 3.91 and 3.65 ± 0.97), (11.33 ± 2.67 and 3.65 ± 0.22) for Groups II, III, and IV, respectively. Meanwhile, the lowest values of the SUVmax and SUVmean among all of the skeletal sites were observed in humerus and ribs (3.22 ± 0.67 and 0.97 ± 0.18), (5.16 ± 1.82 and 1.18 ± 0.16) for Group I, IV and in humerus (3.17 ± 0.58 and 0.85 ± 0.26), (3.98 ± 1.12 and 1.04 ± 0.28) for Group II and III, respectively. Detailed average normal SUVmax and SUVmean values for different skeletal sites are mentioned in Table 4.

Although overall COV values of SUVmax were comparably lower in Group II in contrast to rest imaging groups, the overall COV values of SUVmean were comparably lower in Group IV in contrast to rest groups. The highest COV values of the SUVmax and SUVmean among all of the skeletal sites were observed in sternum and femur (0.39 and 0.32) for Group I and in the skull (0.34 and 0.35), (0.45 and 0.45), (0.40 and 0.40) for Groups II, III, and IV, respectively. Meanwhile, the lowest COV values of the SUVmax and SUVmean among all of the skeletal sites

Table 3: Comparison of different demographic, clinical and injection parameters between imaging groups

Parameter	SPECT/CT imaging groups				*P*
	I (2 h)	II (3 h)	III (4 h)	IV (5 h)	
Age (years)	46.66±10.04	45.4±6.68	44.06±9.56	51.6±15.19	>0.46
BMI	22.38±2.94	21.92±2.97	21.54±2.91	22.63±2.67	>0.89
ALP (IU/L)	77.6±16.11	78.26±9.42	75.26±13.81	80.26±16.75	>0.84
Creatinine (mg/dL)	0.69±0.14	0.65±0.11	0.66±0.11	0.67±0.10	>0.82
Administered activity (MBq)	921.99±10.44	922.28±12.06	922.95±12.43	921.86±9.89	>0.99

Results displayed as mean±SD (range). SPECT/CT: Single photon emission computed tomography/computed tomography, BMI: Body mass index, ALP: Alkaline phosphatase, SD: Standard deviation

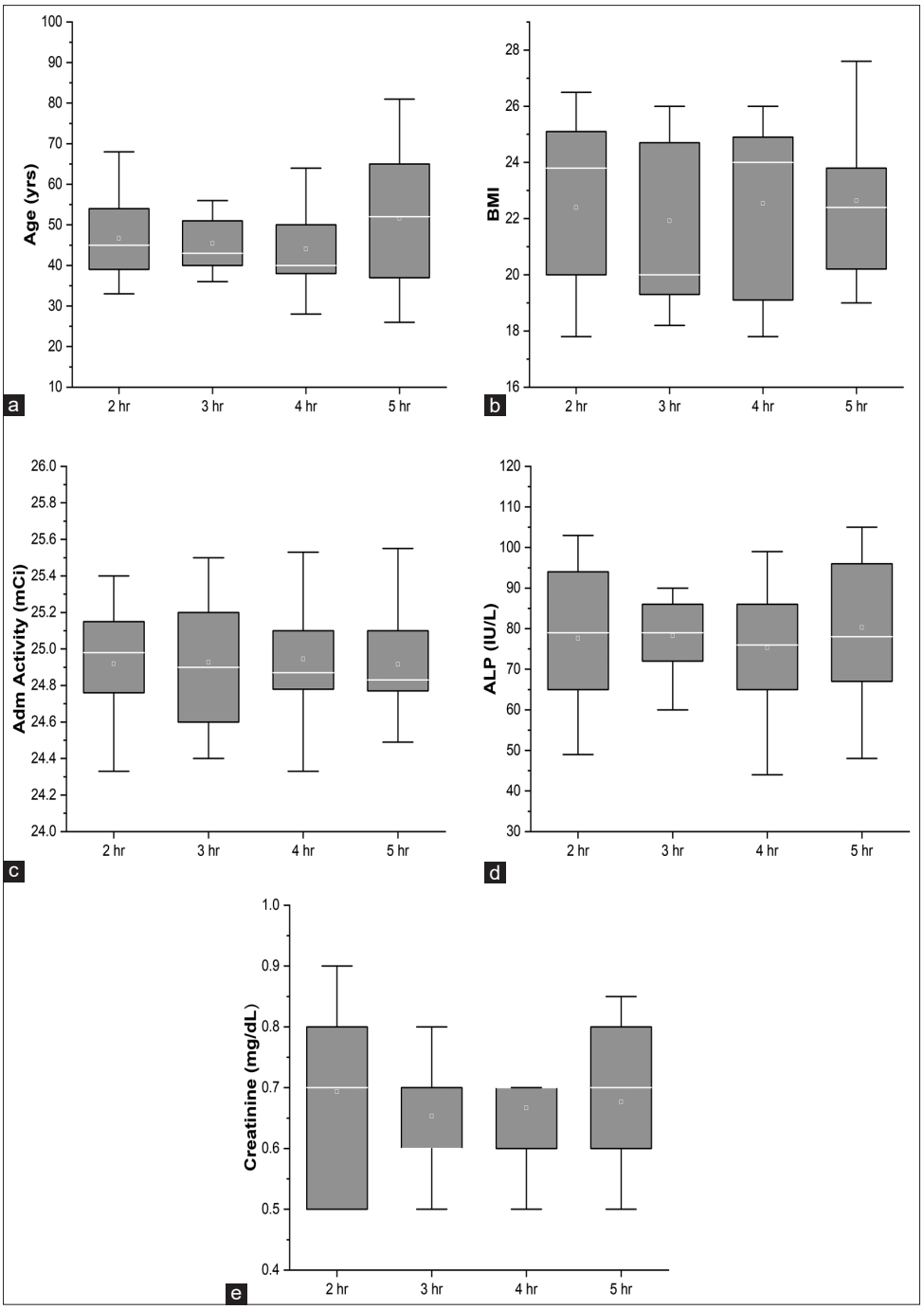

Figure 3: Comparison of baseline parameters between imaging groups. No significant difference noted in age (a) *P* = 0.46, BMI (b) *P* = 0.89, administered activity (c) *P* = 0.99, ALP (d) *P* = 0.84 and creatinine (e) *P* = 0.82 between all four groups. BMI, body mass index; ALP, alkaline phosphatase

were observed in cervical and pelvis (0.08 and 0.16) for Group I, scapula and pelvis (0.08 and 0.13) for Group II, scapula (0.13 and 0.12) for Group III, and in ribs and thoracic (0.05 and 0.06) for Group IV, respectively. Detailed COV values for each skeletal site are also mentioned in Table 4.

Comparison of SUVs for each skeletal site between groups shows an increase in SUVmax and SUVmean value with postinjection acquisition time [Figures 6-9]. As per our observation, IIIrd and IVth imaging groups relatively show higher SUVs as compared to the rest imaging groups. We have observed a significant difference ($P < 0.05$) in SUVmax for sternum, cervical, humerus, ribs, and pelvis sites concerning time. However, a significant difference ($P < 0.05$) was noted in SUVmean for all skeletal sites concerning time.

Tables 5-8 show the relation between the SUVs and age, BMI, administered activity and ALP. All SUVs of different

Table 4: Comparison of maximum standardized uptake value, standardized uptake value mean, coefficient of variation of different imaging groups for normal skeletal sites in breast cancer patients

Skeletal site	SPECT/CT imaging groups				*P*
	I (2 h)	II (3 h)	III (4 h)	IV (5 h)	
Skull					
SUVmax	4.39±0.90	4.4±1.51	5.3±2.43	6.04±2.43	0.25
SUVmean	1.13±0.31	1.35±0.38	1.58±0.72	1.99±0.80	0.03
COV SUVmax	0.2	0.34	0.45	0.4	
COV SUVmean	0.27	0.35	0.45	0.4	
Sternum					
SUVmax	4.7±1.84	5.32±1.15	6.97±2.05	8.73±1.91	0.0001
SUVmean	1.64±0.32	2.19±0.32	2.95±0.57	2.98±0.54	0.0001
COV SUVmax	0.39	0.21	0.29	0.21	
COV SUVmean	0.19	0.14	0.19	0.18	
Cervical					
SUVmax	6.92±0.60	7.74±0.96	8.37±1.59	10.18±2.19	0.0001
SUVmean	2.45±0.61	2.67±0.41	3.05±0.44	3.32±0.55	0.0003
COV SUVmax	0.08	0.12	0.19	0.21	
COV SUVmean	0.25	0.15	0.14	0.16	
Thoracic					
SUVmax	8.34±2.20	8.07±1.29	9.09±1.87	9.37±1.57	0.23
SUVmean	2.89±0.58	3.04±0.64	3.65±0.97	3.65±0.22	0.001
COV SUVmax	0.26	0.16	0.2	0.16	
COV SUVmean	0.2	0.21	0.26	0.06	
Lumbar					
SUVmax	8.89±2.26	8.16±1.49	9.34±2.15	9.57±2.05	0.21
SUVmean	2.83±0.63	2.9±0.53	3.61±0.93	3.44±0.31	0.006
COV SUVmax	0.25	0.18	0.23	0.21	
COV SUVmean	0.22	0.18	0.25	0.09	
Scapula					
SUVmax	7.2±0.82	6.92±0.61	7.6±1.04	7.47±0.98	0.24
SUVmean	1.26±0.26	1.17±0.33	1.72±0.22	1.88±0.19	0.0002
COV SUVmax	0.11	0.08	0.13	0.13	
COV SUVmean	0.21	0.28	0.12	0.1	
Humerus					
SUVmax	3.22±0.67	3.17±0.58	3.98±1.12	5.16±1.82	0.0002
SUVmean	1.06±0.22	0.85±0.26	1.04±0.28	1.24±0.39	0.03
COV SUVmax	0.21	0.18	0.28	0.35	
COV SUVmean	0.21	0.31	0.27	0.31	
Femur					
SUVmax	4.76±1.69	4.92±1.45	5.56±2.37	5.79±2.15	0.32
SUVmean	1.24±0.40	1±0.30	1.34±0.34	1.82±0.45	0.0001
COV SUVmax	0.35	0.29	0.42	0.37	
COV SUVmean	0.32	0.3	0.25	0.25	
Ribs					
SUVmax	5.48±1.08	5.14±0.42	6.39±0.94	7.53±0.42	0.0004
SUVmean	0.97±0.18	0.92±0.21	1.16±0.20	1.18±0.16	0.0001
COV SUVmax	0.19	0.08	0.14	0.05	
COV SUVmean	0.19	0.23	0.17	0.13	
Pelvis					
SUVmax	8.83±1.57	9.6±1.32	10.93±3.91	11.33±2.67	0.03
SUVmean	2.68±0.43	2.86±0.37	3.34±0.75	3.29±0.41	0.002
COV SUVmax	0.17	0.13	0.35	0.23	
COV SUVmean	0.16	0.13	0.22	0.12	

Results displayed as mean±SD. SUV: Standardized uptake value, COV: Coefficient of variation, SUVmax: Maximum standardized uptake value, SD: Standard deviation, SPECT/CT: Single photon emission computed tomography/computed tomography

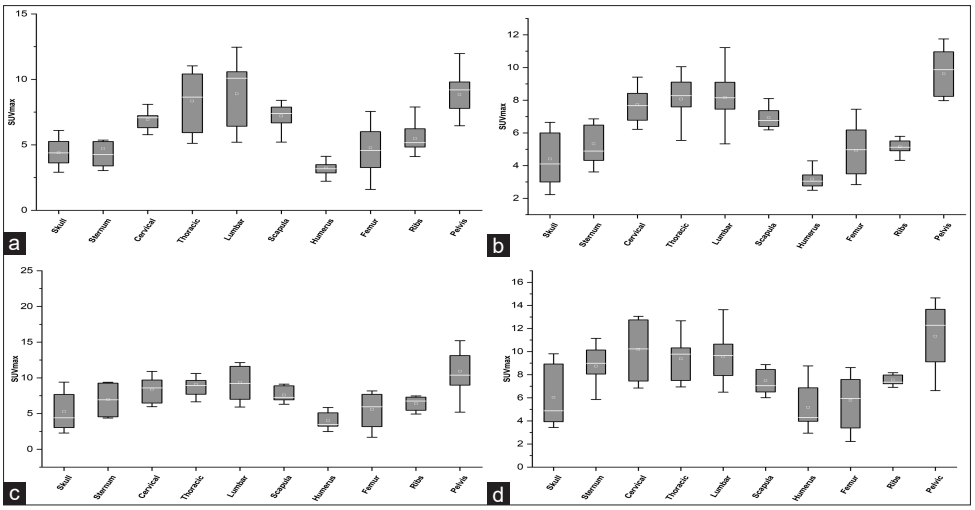

Figure 4: Distribution of SUVmax values quantified in Group I (a), Group II (b), Group III (c), and Group IV (d). The top and bottom of the boxes represented the first and third quartile, end of whiskers represented minimum and maximum values of data and horizontal line inside the boxes represent median. SUVmax, maximum standardized uptake value

Table 5: Correlation coefficients (*r*) between standardized uptake values and age

Skeletal site	SPECT/CT imaging groups			
	I (2 h)	II (3 h)	III (4 h)	IV (5 h)
Skull				
SUVmax	0.46	0.1	0.33	0.35
SUVmean	0.32	0.41	0.14	0.27
Sternum				
SUVmax	0. 22	0.12	0.09	0.53
SUVmean	0.48	0.25	0.37	0.11
Cervical				
SUVmax	0.22	0.43	−0.12	0.28
SUVmean	−0.33	0.43	0.21	0.24
Thoracic				
SUVmax	−0.22	0.1	0.11	−0.73
SUVmean	−0.45	0.12	0.46	0.22
Lumbar				
SUVmax	−0.39	−0.04	0.04	−0.19
SUVmean	−0.47	−0.1	0.38	−0.02
Scapula				
SUVmax	0.46	0.17	0.57	0.41
SUVmean	0.0013	0.07	−0.04	0.24
Humerus				
SUVmax	−0.03	−0.3	−0.02	0.33
SUVmean	0.08	0.11	−0.23	0.33
Femur				
SUVmax	−0.27	0.18	0.07	−0.44
SUVmean	−0.2	0.09	0.42	−0.08
Ribs				
SUVmax	0.11	−0.05	0.009	−0.29
SUVmean	−0.12	0.05	−0.22	−0.04
Pelvis				
SUVmax	−0.54	0.04	−0.35	−0.58
SUVmean	−0.44	0.04	−0.08	−0.08

SUV: Standardized uptake value, SUVmax: Maximum standardized uptake value, SPECT/CT: Single photon emission computed tomography/computed tomography

Table 6: Correlation coefficients (*r*) between standardized uptake values and body mass index

Skeletal site	SPECT/CT imaging groups			
	I (2 h)	II (3 h)	III (4 h)	IV (5 h)
Skull				
SUVmax	0.38	−0.54	0.37	0.35
SUVmean	0.34	0.46	0.18	0.26
Sternum				
SUVmax	0. 24	0.16	0.1	0.57
SUVmean	−0.46	−0.28	0.38	0.21
Cervical				
SUVmax	0.55	0.07	−0.39	−0.51
SUVmean	−0.47	−0.12	−0.05	−0.14
Thoracic				
SUVmax	−0.24	0.14	0.05	0.47
SUVmean	−0.18	−0.08	0.47	−0.11
Lumbar				
SUVmax	0.46	0.33	0.08	0.4
SUVmean	−0.43	−0.16	−0.4	−0.06
Scapula				
SUVmax	0.41	0.22	0.61	0.41
SUVmean	0.012	0.06	0.06	0.27
Humerus				
SUVmax	−0.17	0.45	−0.16	0.67
SUVmean	0.07	0.16	−0.25	0.35
Femur				
SUVmax	−0.26	−0.15	0.22	−0.59
SUVmean	0.44	0.17	0.46	0.28
Ribs				
SUVmax	0.23	−0.08	−0.07	−0.32
SUVmean	−0.18	−0.08	−0.27	−0.08
Pelvis				
SUVmax	0.25	0.47	−0.16	0.24
SUVmean	−0.39	0.49	0.26	0.31

SUV: Standardized uptake value, SUVmax: Maximum standardized uptake value, SPECT/CT: Single photon emission computed tomography/computed tomography

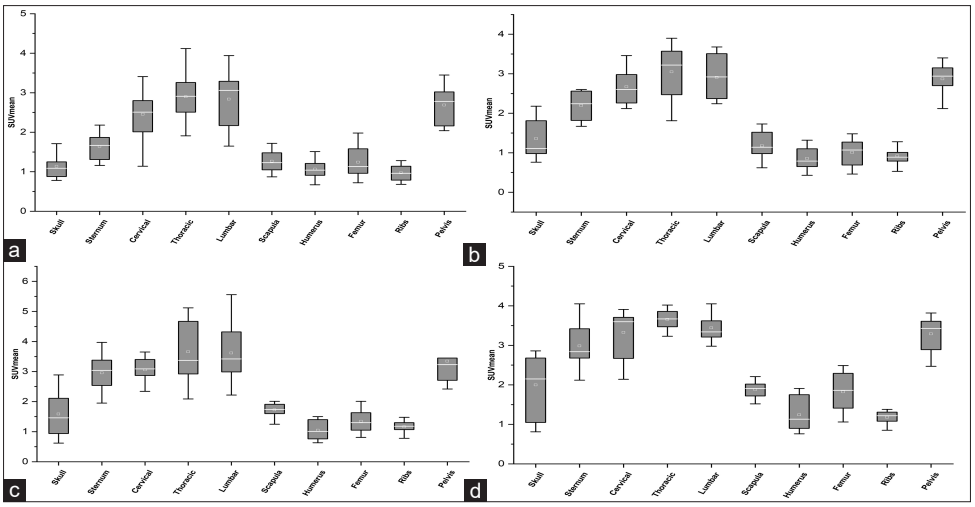

Figure 5: Distribution of SUVmean values quantified in Group I (a), Group II (b), Group III (c), and Group IV (d). The top and bottom of the boxes represented the first and third quartile, end of whiskers represented minimum and maximum values of data and horizontal line inside the boxes represent median. SUVmean, mean standardized uptake value

Table 7: Correlation coefficients (*r*) between standardized uptake values and administered activity

Skeletal site	SPECT/CT imaging groups			
	I (2 h)	II (3 h)	III (4 h)	IV (5 h)
Skull				
SUVmax	−0.27	−0.31	0.21	0.06
SUVmean	0.006	−0.2	0.3	0.27
Sternum				
SUVmax	−0.3	−0.14	0.14	0.33
SUVmean	−0.32	0.71	−0.06	0.32
Cervical				
SUVmax	−0.12	0.27	0.18	0.37
SUVmean	−0.39	−0.45	0.01	0.39
Thoracic				
SUVmax	−0.04	−0.2	0.36	−0.01
SUVmean	−0.42	−0.27	0.3	0.37
Lumbar				
SUVmax	−0.32	0.007	0.14	0.3
SUVmean	−0.17	0.58	0.22	−0.13
Scapula				
SUVmax	0.16	0.09	0.56	0.38
SUVmean	−0.51	−0.3	0.19	−0.004
Humerus				
SUVmax	−0.1	−0.3	0.21	−0.15
SUVmean	0.01	−0.71	0.09	0.45
Femur				
SUVmax	−0.16	−0.24	0.16	−0.41
SUVmean	−0.24	0.25	0.07	0.14
Ribs				
SUVmax	−0.2	0.32	0.19	0.39
SUVmean	0.1	−0.4	−0.07	0.37
Pelvis				
SUVmax	−0.72	0.25	0.21	−0.37
SUVmean	−0.48	0.18	0.32	0.56

SUV: Standardized uptake value, SUVmax: Maximum standardized uptake value, SPECT/CT: Single photon emission computed tomography/computed tomography

Table 8: Correlation coefficients (*r*) between standardized uptake values and alkaline phosphatase

Skeletal site	SPECT/CT imaging groups			
	I (2 h)	II (3 h)	III (4 h)	IV (5 h)
Skull				
SUVmax	−0.05	−0.38	−0.27	−0.004
SUVmean	0.006	0.18	0.28	0.21
Sternum				
SUVmax	−0.75	0.27	0.24	−0.33
SUVmean	−0.49	0.15	0.35	0.51
Cervical				
SUVmax	0.16	0.29	0.28	0.31
SUVmean	−0.21	−0.51	0.09	−0.32
Thoracic				
SUVmax	−0.21	0.35	0.22	0.31
SUVmean	0.15	−0.38	−0.15	0.41
Lumbar				
SUVmax	−0.08	−0.76	0.13	−0.17
SUVmean	−0.27	−0.51	0.21	−0.13
Scapula				
SUVmax	0.26	0.03	0.51	0.45
SUVmean	−0.61	−0.26	0.12	0.06
Humerus				
SUVmax	−0.22	−0.78	0.27	0.13
SUVmean	0.14	0.49	0.16	0.42
Femur				
SUVmax	−0.18	−0.22	−0.08	−0.48
SUVmean	−0.23	−0.21	0.18	0.19
Ribs				
SUVmax	−0.08	−0.25	0.42	−0.28
SUVmean	−0.46	−0.32	0.35	0.31
Pelvis				
SUVmax	−0.29	−0.21	0.24	0.29
SUVmean	−0.38	−0.72	−0.09	0.37

SUV: Standardized uptake value, SUVmax: Maximum standardized uptake value, SPECT/CT: Single photon emission computed tomography/computed tomography

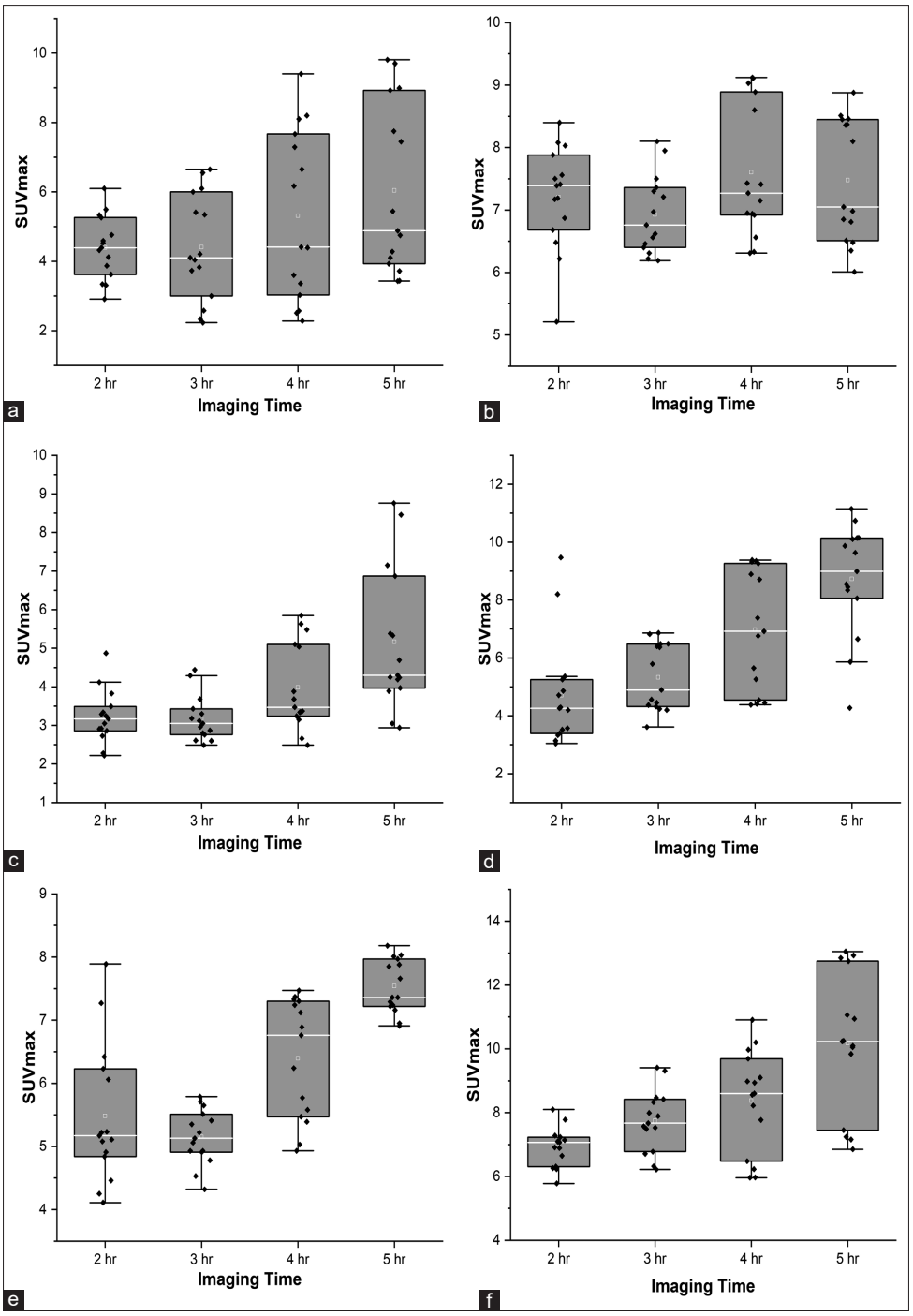

Figure 6: Box and whiskers plot showing the distribution of SUVmax values in patient groups; (a) skull (*P* = 0.25), (b) scapula (*P* = 0.24), (c) humerus (*P* = 0.0002), (d) sternum (*P* = 0.0001), (e) ribs (*P* = 0.0004) and (f) cervical (*P* = 0.0001). The top and bottom of the boxes represented the first and third quartile, end of whiskers represented minimum and maximum values of data and horizontal line inside the boxes represent median. SUVmax, maximum standardized uptake value

imaging groups show weak and no significant correlation with age, BMI, administered activity and ALP.

Discussion

Technological evolution and advances in molecular imaging have made quantitative measurements vastly important in the staging of various diseases, differentiation of metastasis from degenerative changes, and also in the evaluation of various treatment responses.[30] The advancement in reconstruction algorithms and the use of various corrections techniques have made SPECT feasible as similar to PET for the quantification.[6,31] A major challenge with SPECT/CT is the reduction of total acquisition time. However, recent studies reveal that bone

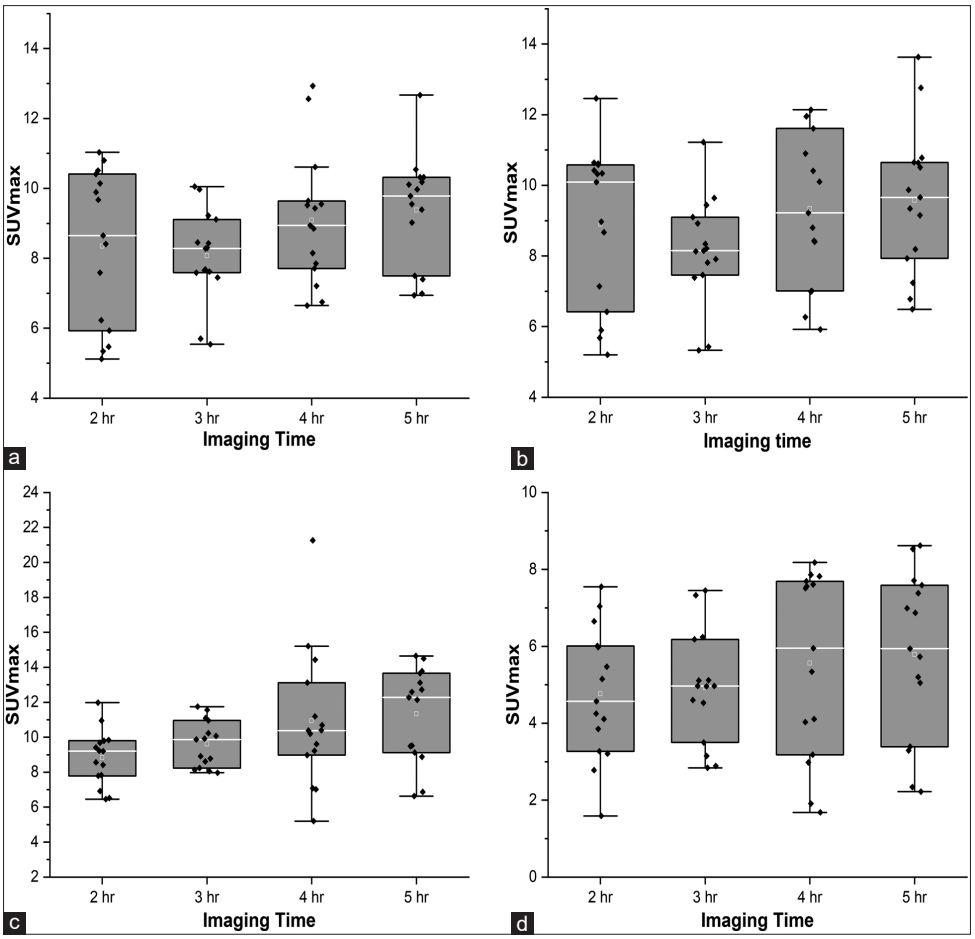

Figure 7: Box and whiskers plot showing the distribution of SUVmax values in patient groups; (a) thoracic (*P* = 0.23), (b) lumber (*P* = 0.21), (c) pelvis (*P* = 0.03) and (d) femur (*P* = 0.32). The top and bottom of the boxes represented the first and third quartile, end of whiskers represented minimum and maximum values of data and horizontal line inside the boxes represent median. SUVmax, maximum standardized uptake value

SPECT/CT is diagnostically equal to NaF PET/CT and the imaging can also be executed with low acquisition time.[32,33] There are no studies that reported the normal SUV values for various skeletal sites using Tc-99m MDP SPECT/CT bone scan on breast cancer patients having no metastatic or degenerative bone diseases. Moreover, this is the first study to demonstrate time-dependent changes on normal SUVs with SPECT/CT.

The results of our study show wide variability in different normal SUV values for various skeletal sites. Here we evaluated different SUVs including SUVmax and SUVmean based on patient BW, which is the most popular method. However, SUVmean is being used as useful alternatives because of the limitations of SUVmax, which is restrictive to noise and statistical changes in data.[34] In our study, the values of SUVmax and SUVmean of all groups were relatively higher in thoracic, lumbar and pelvis as compared to ribs, humerus, and femur. Our results are supported by the results of Win AZ and Aparici CM, which suggested the highest SUV values in vertebrae as compared to humerus and femur.[22] The most likely reason being that higher trabecular density bones show higher blood flow and metabolism lead to higher uptake values.[35-38] Furthermore, weight-bearing and excess mechanical stress bones such as thoracic vertebra, lumber vertebra, and pelvic bones enhance osteoblastic activity lead to higher uptake.[39] Another fluoride-based PET study also revealed that cortical bone-like humerus usually has a lower level of bone metabolism, whereas lumbar spine is excess in trabecular bone.[40]

The phosphonate group of MDP tend to have lesser accumulation in the hydroxyapatite structure of the appendicular skeleton (e.g. humerus and femur) than in the axial skeleton (e.g. vertebrae and pelvis). Win and Aparici measured SUVmax values from Na18F PET/CT studies performed at 60 min postinjection on 11 patients free of cancer or any metabolic disease.[22] Their results were found in good agreement with our study results predominantly for Group II. Here, we observed <10% difference in SUVmax values for skeletal sites, i.e. cervical, thoracic, lumber, and sternum. The differences in SUVs can be resulted from differences in instrumentation, acquisition parameters, and reconstruction techniques.[41] In our study, highest mean SUV value was found in thoracic spine for all four groups. A study by Li *et al*. suggested that the SUVmean values in the humerus and femur are around 15%–25% of the total value in the spine.[42] However, mean SUV values in the

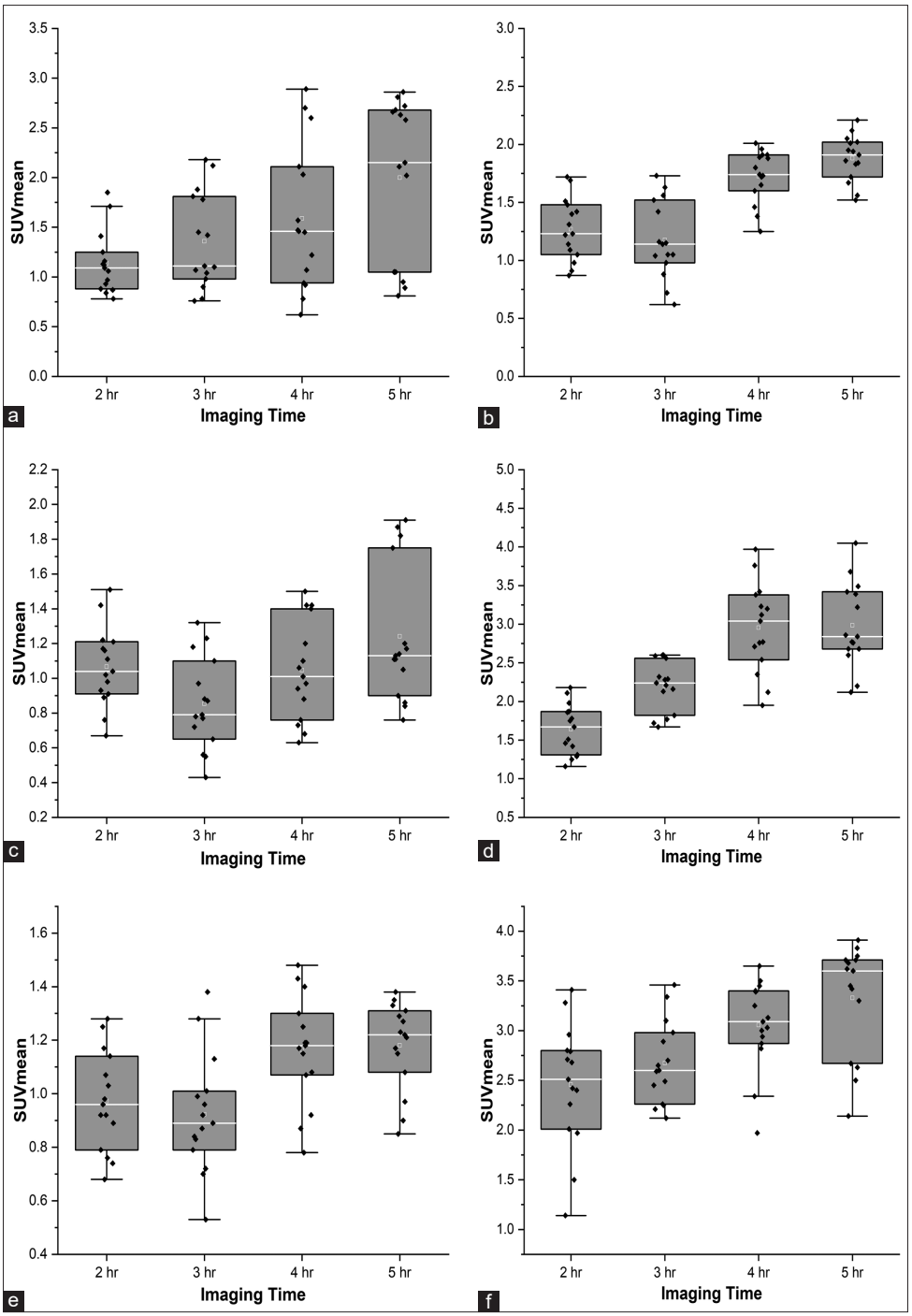

Figure 8: Box and whiskers plot showing the distribution of SUVmean values in patient groups; (a) skull (*P* = 0.03), (b) scapula (*P* = 0.0002), (c) humerus (*P* = 0.03), (d) sternum (*P* = 0.0001), (e) ribs (*P* = 0.0001) and (f) cervical (*P* = 0.0003). The top and bottom of the boxes represented the first and third quartile, end of whiskers represented minimum and maximum values of data and horizontal line inside the boxes represent median. SUVmean, mean standardized uptake value

humerus and femur for Group II were found marginally higher in our study, which falls within 25%–35% of value in the thoracic spine (3.04). Meanwhile, values in the humerus and femur for rest imaging groups fall within 35%–45% of value in thoracic spine. Moreover, we have found that SUVmax values in the humerus and femur for all four groups fall within a range of 40%–60% of the total value in the thoracic spine.

In the present study, the SUVmean value for normal pelvis in all imaging groups was also found lower than thoracic and lumbar vertebra. A study by Kaneta *et al*. found SUV mean values of pelvis lower than vertebral body.[3] Furthermore, Wang *et al*. demonstrated normal SUVmax and mean value in the normal pelvis which was 3.8 and 2.07, respectively.[7] Our study results reveal SUVmean value in the normal pelvis of Group II is about

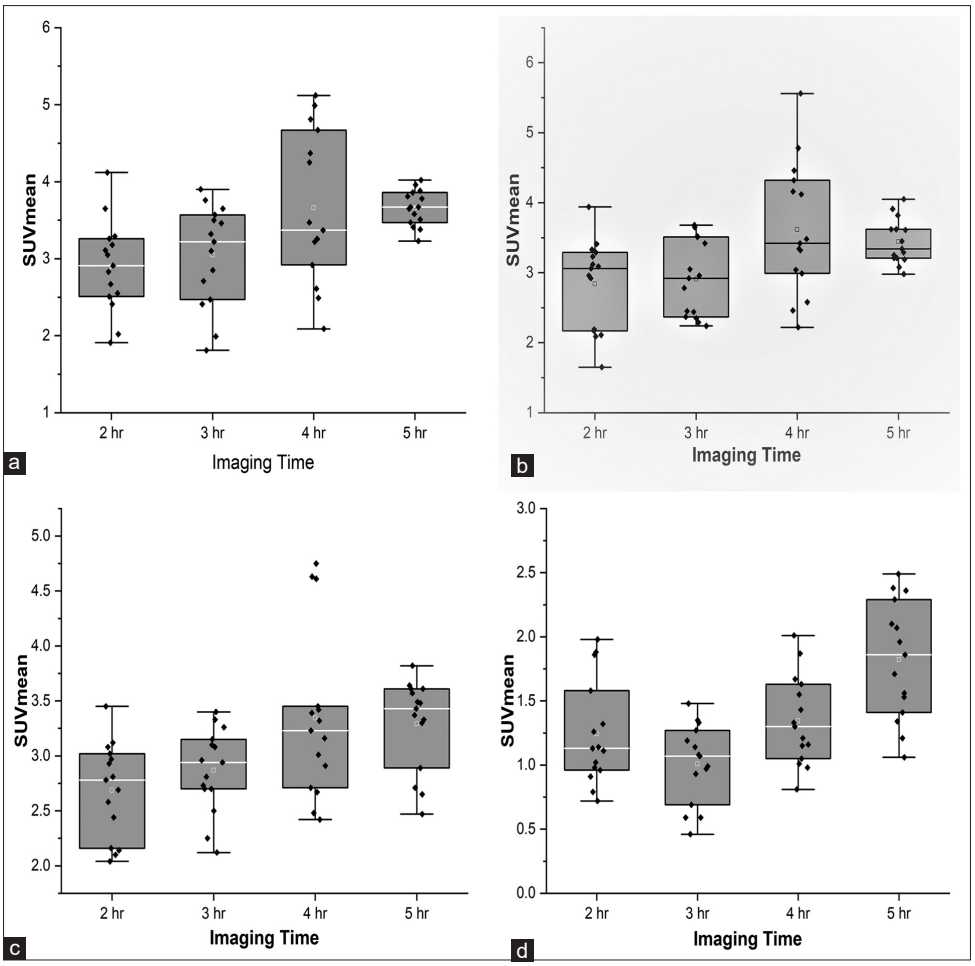

Figure 9: Box and whiskers plot showing the distribution of SUVmean values in patient groups; (a) thoracic (*P* = 0.001), (b) lumber (*P* = 0.006), (c) pelvis (*P* = 0.002), and (d) femur (*P* = 0.0001). The top and bottom of the boxes represented the first and third quartile, end of whiskers represented minimum and maximum values of data and horizontal line inside the boxes represent median. SUVmean, mean standardized uptake value

2.86 which were found in the same extent as obtained by them. Meanwhile, we have observed higher SUVmax values in pelvis about 9.6 as compared to their results. The possible reason is the technique used for delineation of VOI in pelvis images, where we included the sacroiliac joint as a part of the pelvic surface. Another study also revealed SUVmax and SUVmean values in vertebrae with 6.51 and 3.92, respectively.[8] Although their results were in good accordance with our SUV results in Group II, which were about 7.99 and 2.87, respectively. Moreover, these values were also observed as compared to previously reported SUVs for normal vertebrae, for example, 7.1 ± 0.4 and 7.6 ± 2.4 for SUVmax, and 4.4 ± 0.5, 4.6 ± 1.7, and 5.9 ± 1.5 for SUVmean.[3,43,44]

We used COV to see the dispersion in SUV values for different skeletal sites. It is known that the lower the COV value, the more accurate the measurement. SUVmax values in Group II, which was acquired at a standard time of 3 h postinjection showed less COV as compared to the rest imaging groups. We observed lower dispersion in SUV for all skeletal sites except the skull bone. Furthermore, our results demonstrate lower COV values of SUVmax at vertebral level in Group II, suggesting the smallest dispersion as compared to SUVmean values. Our results are supported by the findings of Kaneta *et al*.[3]

Our study results show changes in SUVs concerning postinjection acquisition time. As the acquisition time is increasing, SUV difference is also increasing between imaging groups. Moreover, the highest differences in SUVs were found between Groups I and IV. We hypothesized that this is due to progressive changes in bone to background uptake ratio over a while.[45] The influence of postinjection acquisition time on SUVs has already been studied in PET/CT.[25-27,46] Our results were supported by a study where a percentage of activity retained in the background tissue decreased from 54.1% at 1 h postinjection to 22.4% at 4 h, whereas uptake of Tc-99m MDP in bone increased from 14.6% to 24.7%. Although, in the same period, urinary excretion of Tc-99m MDP was also increased from 31.3% to 52.9%.[47,48]

In our study, we did not find any significant relation between SUVs and patient parameters, i.e. age, BMI,

administered activity, and ALP. Our results were found in contrast with previous reports.[3,7,8] The main limitations of our study are the small sample size and differences in the target population in each imaging group. Moreover, SUV measurements from the entirely healthy population without any malignancy were not obtained. Therefore, in the future comparative study of SUVs at different times after injection can be performed in a larger population having the same subjects to better characterize the SUV for normal skeletal sites.

Conclusions

We concluded that Tc-99m MDP SPECT/CT is a feasible and viable option to quantify SUVs in normal skeletal sites. Our study shows variability in normal SUV values for different skeletal sites in breast cancer patients. Vertebral bodies and pelvis contribute the highest SUV values. If normal SUV values for metastatic prone skeletal sites are known, they can be used as a biomarker in the identification of disease level and the evaluation of treatment response and follow-up to cancer and other bone diseases. Furthermore, we concluded that SUVs change with postinjection acquisition time. The time dependency of SPECT/CT SUVs emphasizes the usefulness of routinely acquired images at the same time after Tc-99m MDP injection, especially in follow-up studies. However, more studies and references are needed to implement SUVs of bone in routine clinical practice.

Financial support and sponsorship

Nil.

Conflicts of interest

There are no conflicts of interest.

References

1. Abdelrazek S, Szumowski P, Rogowski F, Kociura-Sawicka A, Mojsak M, Szorc M. Bone scan in metabolic bone diseases. Review. Nucl Med Rev Cent East Eur 2012;15:124-31.
2. Adams C, Banks KP. Bone scan. In: StatPearls. Treasure Island (FL): Starpearls Publishing; 2020.
3. Kaneta T, Ogawa M, Daisaki H, Nawata S, Yoshida K, Inoue T. SUV measurement of normal vertebrae using SPECT/CT with Tc-99m methylene diphosphonate. Am J Nucl Med Mol Imaging 2016;6:262-8.
4. Macedo F, Ladeira K, Pinho F, Saraiva N, Bonito N, Pinto L, *et al.* Bone metastases: An overview. Oncol Rev 2017;11:321.
5. Wale DJ, Wong KK, Savas H, Kandathil A, Piert M, Brown RK. Extraosseous findings on bone scintigraphy using fusion SPECT/CT and correlative imaging. AJR Am J Roentgenol 2015;205:160-72.
6. Bailey DL, Willowson KP. An evidence-based review of quantitative SPECT imaging and potential clinical applications. J Nucl Med 2013;54:83-9.
7. Wang R, Duan X, Shen C, Han D, Ma J, Wu H, *et al*. A retrospective study of SPECT/CT scans using SUV measurement of the normal pelvis with Tc-99m methylene diphosphonate. J Xray Sci Technol 2018;26:895-908.
8. Rohani MF, Yonan SN, Tagiling N, Zainon WM, Udin Y, Nawi NM. Standardized uptake value from semiquantitative bone single-photon emission computed tomography/computed tomography in normal thoracic and lumbar vertebrae of breast cancer patients. Asian Spine J 2020;14:629-38.
9. Arvola S, Jambor I, Kuisma A, Kemppainen J, Kajander S, Seppänen M, *et al.* Comparison of standardized uptake values between (99m) Tc-HDP SPECT/CT and (18) F-NaF PET/CT in bone metastases of breast and prostate cancer. EJNMMI Res 2019;9:6.
10. Bailey DL, Willowson KP. Quantitative SPECT/CT: SPECT joins PET as a quantitative imaging modality. Eur J Nucl Med Mol Imaging 2014;41 Suppl 1:S17-25.
11. Seo Y, Wong KH, Sun M, Franc BL, Hawkins RA, Hasegawa BH. Correction of photon attenuation and collimator response for a body-contouring SPECT/CT imaging system. J Nucl Med 2005;46:868-77.
12. O'Connor MK, Kemp BJ. Single-photon emission computed tomography/computed tomography: Basic instrumentation and innovations. Semin Nucl Med 2006;36:258-66.
13. Brenner W, Vernon C, Muzi M, Mankoff DA, Link JM, Conrad EU, *et al.* Comparison of different quantitative approaches to 18F-fluoride PET scans. J Nucl Med 2004;45:1493-500.
14. Nestle U, Kremp S, Schaefer-Schuler A, Sebastian-Welsch C, Hellwig D, Rübe C, *et al*. Comparison of different methods for delineation of 18F-FDG PET-positive tissue for target volume definition in radiotherapy of patients with non-small cell lung cancer. J Nucl Med 2005;46:1342-8.
15. Even-Sapir E, Mishani E, Flusser G, Metser U. 18F-Fluoride positron emission tomography and positron emission tomography/computed tomography. Semin Nucl Med 2007;37:462-9.
16. Cook G Jr., Parker C, Chua S, Johnson B, Aksnes AK, Lewington VJ. 18F-fluoride PET: Changes in uptake as a method to assess response in bone metastases from castrate-resistant prostate cancer patients treated with 223Ra-chloride (Alpharadin). EJNMMI Res 2011;1:4.
17. Segall G, Delbeke D, Stabin MG, Even-Sapir E, Fair J, Sajdak R, *et al.* SNM practice guideline for sodium 18F-fluoride PET/CT bone scans 1.0. J Nucl Med 2010;51:1813-20.
18. Even-Sapir E, Metser U, Mishani E, Lievshitz G, Lerman H, Leibovitch I. The detection of bone metastases in patients with high-risk prostate cancer: 99mTc-MDP Planar bone scintigraphy, single- and multi-field-of-view SPECT, 18F-fluoride PET, and 18F-fluoride PET/CT. J Nucl Med 2006;47:287-97.
19. Tateishi U, Morita S, Taguri M, Shizukuishi K, Minamimoto R, Kawaguchi M, *et al*. A meta-analysis of (18) F-Fluoride positron emission tomography for assessment of metastatic bone tumor. Ann Nucl Med 2010;24:523-31.
20. Lima GM, Diodato S, Costabile E, Cicoria G, Civollani S, Marchetti C, *et al.* Low dose radiation 18F-fluoride PET/CT in the assessment of unilateral condylar hyperplasia of the mandible: Preliminary results of a single centre experience. Eur J Hybrid Imaging 2018;2:7.
21. Oldan JD, Hawkins AS, Chin BB. 18F Sodium Fluoride PET/CT in patients with prostate Cancer: Quantification of normal tissues, benign degenerative lesions, and malignant lesions. World J Nucl Med 2016;15:102-8.
22. Win AZ, Aparici CM. Normal SUV values measured from NaF18-PET/CT bone scan studies. PLoS One 2014;9:e108429.
23. Sabbah N, Jackson T, Mosci C, Jamali M, Minamimoto R, Quon A, *et al.* 18F-sodium fluoride PET/CT in oncology: An atlas of SUVs. Clin Nucl Med 2015;40:e228-31.
24. Suh MS, Lee WW, Kim YK, Yun PY, Kim SE. Maximum

standardized uptake value of (99m) Tc hydroxymethylene diphosphonate SPECT/CT for the evaluation of temporomandibular joint disorder. Radiology 2016;280:890-6.
25. Beaulieu S, Kinahan P, Tseng J, Dunnwald LK, Schubert EK, Pham P, *et al.* SUV varies with time after injection in (18) F-FDG PET of breast cancer: Characterization and method to adjust for time differences. J Nucl Med 2003;44:1044-50.
26. Wang R, Chen H, Fan C. Impacts of time interval on 18F-FDG uptake for PET/CT in normal organs: A systematic review. Medicine (Baltimore) 2018;97:e13122.
27. Adams MC, Turkington TG, Wilson JM, Wong TZ. A systematic review of the factors affecting accuracy of SUV measurements. AJR Am J Roentgenol 2010;195:310-20.
28. Donohoe KJ, Henkin RE, Royal HD, Brown ML, Collier BD, O'Mara RE, *et al*. Procedure guideline for bone scintigraphy: 1.0. Society of Nuclear Medicine. J Nucl Med 1996;37:1903-6.
29. NM Quantification Q. Metrix for SPECT/CT Package. White Paper DOC1951185: GE Healthcare; 2017.
30. Dickson J, Ross J, Vöö S. Quantitative SPECT: The time is now. EJNMMI Phys 2019;6:4.
31. Seo Y, Mari C, Hasegawa BH. Technological development and advances in single-photon emission computed tomography/computed tomography. Semin Nucl Med 2008;38:177-98.
32. Zacho HD, Manresa JA, Aleksyniene R, Ejlersen JA, Fledelius J, Bertelsen H, *et al.* Three-minute SPECT/CT is sufficient for the assessment of bone metastasis as add-on to planar bone scintigraphy: Prospective head-to-head comparison to 11-min SPECT/CT. EJNMMI Res 2017;7:1.
33. Fonager RF, Zacho HD, Langkilde NC, Fledelius J, Ejlersen JA, Haarmark C, *et al.* Diagnostic test accuracy study of 18F-sodium fluoride PET/CT, 99mTc-labelled diphosphonate SPECT/CT, and planar bone scintigraphy for diagnosis of bone metastases in newly diagnosed, high-risk prostate cancer. Am J Nucl Med Mol Imaging 2017;7:218-27.
34. Vanderhoek M, Perlman SB, Jeraj R. Impact of different standardized uptake value measures on PET-based quantification of treatment response. J Nucl Med 2013;54:1188-94.
35. Lavender JP, Khan RA, Hughes SP. Blood flow and tracer uptake in normal and abnormal canine bone: Comparisons with Sr-85 microspheres, Kr-81m, and Tc-99m MDP. J Nucl Med 1979;20:413-8.
36. Johannesdottir F, Thrall E, Muller J, Keaveny TM, Kopperdahl DL, Bouxsein ML. Comparison of non-invasive assessments of strength of the proximal femur. Bone 2017;105:93-102.
37. Vogt MT, Cauley JA, Kuller LH, Nevitt MC. Bone mineraldensity and blood flow to the lower extremities: The study of osteoporotic fractures. J Bone Miner Res 1997;12:283-9.
38. Puri T, Frost ML, Curran KM, Siddique M, Moore AE, Cook GJ, *et al.* Differences in regional bone metabolism at the spine and hip: A quantitative study using (18) F-fluoride positron emission tomography. Osteoporos Int 2013;24:633-9.
39. Kobayashi N, Inaba Y, Tateishi U, Yukizawa Y, Ike H, Inoue T, *et al.* New application of 18F-fluoride PET for the detection of bone remodeling in early-stage osteoarthritis of the hip. Clin Nucl Med 2013;38:e379-83.
40. Frost ML, Siddique M, Blake GM, Moore AE, Schleyer PJ, Dunn JT, *et al.* Differential effects of teriparatide on regional bone formation using (18) F-fluoride positron emission tomography. J Bone Miner Res 2011;26:1002-11.
41. Nakahara T, Daisaki H, Yamamoto Y, Iimori T, Miyagawa K, Okamoto T, *et al.* Use of a digital phantom developed by QIBA for harmonizing SUVs obtained from the state-of-the-art SPECT/CT systems: A multicenter study. EJNMMI Res 2017;7:53.
42. Li Y, Schiepers C, Lake R, Dadparvar S, Berenji GR. Clinical utility of (18) F-fluoride PET/CT in benign and malignant bone diseases. Bone 2012;50:128-39.
43. Cachovan M, Vija AH, Hornegger J, Kuwert T. Quantification of 99mTc-DPD concentration in the lumbar spine with SPECT/CT. EJNMMI Res 2013;3:45.
44. Kuji I, Yamane T, Seto A, Yasumizu Y, Shirotake S, Oyama M. Skeletal standardized uptake values obtained by quantitative SPECT/CT as an osteoblastic biomarker for the discrimination of active bone metastasis in prostate cancer. Eur J Hybrid Imaging 2017;1:2.
45. Makler PT Jr., Charkes ND. Studies of skeletal tracer kinetics. IV. Optimum time delay for Tc-99m (Sn) methylene disphosphonate bone imaging. J Nucl Med 1980;21:641-5.
46. Noto B, Büther F, Auf der Springe K, Avramovic N, Heindel W, Schäfers M, *et al.* Impact of PET acquisition durations on image quality and lesion detectability in whole-body 68Ga-PSMA PET-MRI. EJNMMI Res 2017;7:12.
47. Moore AE, Blake GM, Fogelman I. Quantitative measurements of bone remodeling using 99mTc-methylene diphosphonate bone scans and blood sampling. J Nucl Med 2008;49:375-82.
48. Rudd TG, Allen DR, Hartnett DE. Tc-99m-methylenediphosphonate versus Tc-99m pyrophosphate: Biologic and Clinical comparison. J Nucl Med 1977;18:872-6.